Cell

Leading Edge
Primer

Microscopy-Based High-Content Screening

Michael Boutros,[1,2,*] Florian Heigwer,[1] and Christina Laufer[1]
[1]Division Signaling and Functional Genomics, German Cancer Research Center (DKFZ) and Department of Cell and Molecular Biology, Heidelberg University, Im Neuenheimer Feld 580, 69120 Heidelberg, Germany
[2]German Cancer Consortium (DKTK), 69120 Heidelberg, Germany
*Correspondence: m.boutros@dkfz.de
http://dx.doi.org/10.1016/j.cell.2015.11.007

Image-based screening is used to measure a variety of phenotypes in cells and whole organisms. Combined with perturbations such as RNA interference, small molecules, and mutations, such screens are a powerful method for gaining systematic insights into biological processes. Screens have been applied to study diverse processes, such as protein-localization changes, cancer cell vulnerabilities, and complex organismal phenotypes. Recently, advances in imaging and image-analysis methodologies have accelerated large-scale perturbation screens. Here, we describe the state of the art for image-based screening experiments and delineate experimental approaches and image-analysis approaches as well as discussing challenges and future directions, including leveraging CRISPR/Cas9-mediated genome engineering.

Introduction

For over a century, genetic screens have attempted to classify mutations on the basis of visual phenotypes, perhaps initiating with Thomas Hunt Morgan, who at the beginning of the last century identified a spontaneous mutation in *Drosophila melanogaster* that produced white eyes instead of red eyes (Morgan, 1910). Morgan followed up not only by mapping the mutation to a chromosome but also by using X-ray radiation to induce mutations and then analyzing the phenotypic consequences and inheritance patterns, thereby laying the foundation of modern genetics.

Complex visual phenotypes have subsequently been deployed to systematically identify genes involved in embryonic development (Nüsslein-Volhard and Wieschaus, 1980) and to identify genes that enhance or suppress known mutations (e.g., Karim et al., 1996) (Figure 1A). Genetic screens for visual phenotypes have been among the most successful genetic approaches used over the past few decades (Bier, 2005; St Johnston, 2002). In particular, the richness and complexity of visual phenotypes are important factors in determining the specificity of a gene's effect, and visual phenotypes are an important tool for classifying genes by similarity into pathways and processes.

Over the past two decades, major technological advances have enabled automated microscopy screens for visual phenotypes in cells and organisms. Cell-based assays have been used to screen large libraries of small molecules to identify potential drug candidates or to characterize gene function through RNAi or genetic perturbations (Boutros and Ahringer, 2008; Carpenter, 2007). Although such phenotypic high-throughput screens first relied on relatively simple assays, such as cell growth and viability or levels of luminescence reporter genes (Boutros et al., 2004; Lum et al., 2003), automated microscopy has opened new avenues for analyzing a broad spectrum of phenotypes. Image-based assays can be used to answer many cell-biological questions. For example, markers for stem cell and differentiation pathways can be used to dissect processes required for stem cell maintenance. Image-based assays can also be used to measure complex cell-morphology phenotypes to classify perturbations according to changes in cell shape and cell behavior (Kiger et al., 2003; Liu et al., 2009).

In this Primer, we discuss the current state of the art of phenotypic screening in cells. We first describe different approaches to cell-based high-content screening, then cover the design and execution of screening experiments as well as data analysis and exploration. We highlight advances in fluorescence-labeling techniques and opportunities to use genome engineering to create novel markers for image-based screens.

What Defines and Enables High-Throughput and High-Content Screens?

In their simplest form, high-throughput screens are cell based and measure a signal averaged over all cells within a microplate well. The signal might be expression of a reporter gene or levels of a small molecule such as ATP, and the cells can be assayed following perturbation by RNAi (applied genome-wide or more selectively) or small molecules. Generally the read-out, as it is averaged over the whole well, disregards differences that might exist due to individual cell responses. Homogenous cell-based assays are mostly limited to one or two measurements in parallel, such as two luminescence channels.

In contrast, microscopy-based, high-content assays allow parallel monitoring of multiple cell phenotypes. Cells can be modified to express fluorescently labeled proteins or stained with fluorescent markers to allow visualization of cellular and subcellular phenotypes. To examine cell shape changes under different conditions or perturbations, fluorescent dyes and/or antibodies have been used to stain cells for actin, tubulin, and DNA, for example (Kiger et al., 2003; Mayer et al., 1999) (Figure 1B). Thus, microscopy-based screens facilitate phenotype measurements in individual cells and heterogeneous response analyses,

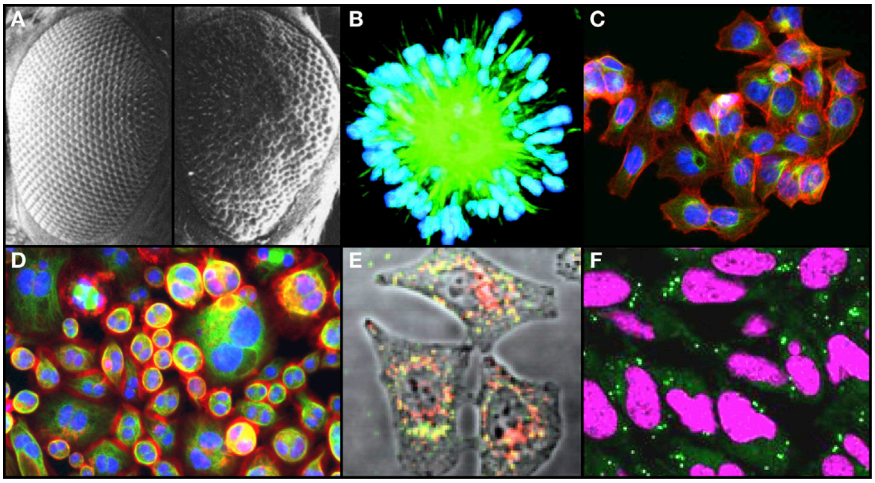

Figure 1. Example High-Content Screens Illustrating the Range of Image-Based Read-outs

(A) Scanning electron micrographs of adult *Drosophila* eyes. Compared to the wild-type (left), a *sev-Ras1*^{V12} transgene led to a rough eye phenotype with misarranged and fused ommatidia. Adapted from Karim et al. (1996).

(B) High-resolution images of BS-C-1 cells stained for DNA (blue) and α-tubulin (green), showing the effect of monastrol treatment on spindle formation. In mitotic cells, monastrol induces a mono-astral microtubule formation. Adapted from Mayer et al. (1999).

(C) HCT116 cells stained for DNA, α-tubulin, and actin to extract quantitative phenotypic features describing cell morphology as described in Laufer et al. (2013).

(D) *Drosophila* cells stained as in (C), imaged at 20× magnification for detailed analysis of morphological phenotypes. RNAi-mediated knockdown of Rho1 leads to enlarged, multi-nucleated cells.

(E) Confocal micrographs of A549 cells infected with influenza A/WSN/33 virus and stained for influenza virus (green) and CD63 (red). Yellow indicates virus particles co-localizing with CD63-labeled late endosomes. Adapted from Karlas et al. (2010).

(F) Confocal micrographs of L cells after treatment with Wnt3a-conditioned medium. Nuclei are stained with DAPI (magenta), and the formation of lipid droplets is visualized with BODIPY 493/503 staining (green). Adapted from Scott et al. (2015).

which provide deeper insights into biological processes (Liberali et al., 2015). For example, heterogeneous viral infections in a cell population have been traced to individual cell states; otherwise, such infections are a masked phenotype in population-averaging experiments (Snijder et al., 2012).

The ability to silence virtually every gene in the genome catalyzed the appeal of systematic visual screening. In addition, major technological advances have expanded the reach of automated screening for visual phenotypes. These advances were driven by improvements in microscopes, such as more stable light sources, faster autofocus, and automation, which led to more advanced automated microscopes. Second, advances in fluorescent probes, new fluorescent protein variants that are used as reporters and fusion proteins, greatly expanded the ability to visualize phenotypes. A third important area includes advances in image-analysis methodologies and the availability of standardized software workflows that greatly reduce the efforts necessary to extract quantitative, multi-parametric information from images (Eliceiri et al., 2012). Together, these methodological advances have brought high-content screening within the reach of many academic laboratories.

Examples of Image-Based Screening

High-content assays can feature very different levels of complexity. In this section, we highlight examples of assays and high-throughput image-based screening experiments (see also Figure 1).

Fluorescent Reporter Genes

Image-based screens can be used to detect changes in reporter genes using additional data, such as cell number or cell shape, to correlate reporter to generic cell responses (e.g., perturbations that induce cell death). Fluorescent reporter screens have been used to study factors that influence pluripotency marker expression. For example, a POU5F1-GFP reporter human embryonic stem cells (hESCs) cell line has been used to image GFP levels and nuclei after perturbing the cells using a genome-wide short interfering RNA (siRNA) library (Chia et al., 2010). The authors quantified GFP levels and compared them to the number of nuclei per well to exclude hits that reduce general cell viability. Similarly, Desbordes et al. (2008) have imaged Oct4 protein levels to identify small molecules that inhibit the pluripotent state of hESC (Desbordes and Studer, 2013; Desbordes et al., 2008).

Protein Localization

Visual assays are a powerful method for assessing changes in subcellular localization of proteins that are indicative, such as for activating signaling pathways or changes in organelle function. In a screen used to identify novel inhibitors of FOXO/Akt signaling, Link et al. (2009) have used an image-based assay to monitor FOXO protein localization in renal carcinoma cells (Link et al., 2009). They transfected cells to express a tagged version of the FOXO protein, treated cells with a library of small molecules, and visualized FOXO localization changes through antibody staining. This screen identified 242 small-molecule inhibitors (out of a library of >33,000) that blocked FOXO nuclear transport. Similarly, perturbations can be used in cell-based assays to identify genes necessary for processes such as autophagy. In a genome-wide RNAi screen, the co-localization of a Sindbis virus capsid protein and autophago-lysosomes has been detected through automated microscopy, and the authors have identified novel candidate genes necessary for autophagy (Orvedahl et al., 2011).

Image-based screens have also been designed to focus on a limited set of features that are directly related to the aim of the study. For example, to identify host cell factors required for influenza infection cycles, a cell-based assay has been used to monitor infection rate with an antibody directed against the virus, along with a second assay used to measure residual influenza in the supernatant (Karlas et al., 2010) (Figure 1E). Using this approach, Karlas et al. (2010) have screened a genome-wide library of RNAi reagents in human cells for factors that change both phenotypic features. Likewise, Rämö et al. (2014) have

compared multiple high-content viral infection screens to discern specific and potential off-target hits in a kinome-wide dataset for eight different pathogens (Rämö et al., 2014). In another study, the role of Wnt signaling in lipid metabolism has been analyzed by establishing a cell-based assay that monitored intracellular lipid droplets (Figure 1F). Using this approach, the authors have shown that Wnt signaling influences lipid mobilization through endocytosis (Scott et al., 2015). FACS or plate-based cytometers have also been used to generate multi-parametric cell-cycle profiles in genome-wide RNAi screens (Björklund et al., 2006; Kittler et al., 2004).

Complex Morphological Assays

High-content screens can use a broad spectrum of cell-shape markers to identify phenotypic changes in an unbiased manner. The rationale behind these approaches is to use complex phenotypes to classify perturbations through a "guilt-by-association" approach, similar to phenotypic forward genetic screens in organisms. Perturbation often elicits similar phenotypic profiles when the same target or pathway is hit, which, in turn, facilitates grouping of perturbations without specifically knowing the target and action mechanism. For example, Loo et al. (2007) have screened approximately 100 drugs at different concentrations and used cellular morphological markers to classify the drugs (Loo et al., 2007). Similarly, Young et al. (2008) have screened 6,000 small molecules and clustered compounds by similarity to infer the mechanism (Young et al., 2008). In a further example, Fuchs et al. (2010) have screened a genome-scale RNAi library and clustered genes by phenotypic similarity, using a 13-dimension feature vector that represented phenotypes visualized by actin, tubulin, and DNA fluorescent stains (Fuchs et al., 2010).

Fluorescent-tag labeling for proteins can also be used to visualize complex phenotypes in image-based screens. In budding yeast, Vizeacoumar et al. (2010) have introduced GFP-tagged tubulin and genetically crossed this strain with a library of deletion strains (Vizeacoumar et al., 2010). Using automated imaging and image analysis to segment subcellular objects, the authors calculated multiple quantitative phenotypic features, including spindle-axis orientation and distance to the budding site.

To map gene-gene interactions, Fischer et al. (2015) have used double RNAi and image-based phenotyping to generate a large genetic interaction map for 21 phenotypic features in *Drosophila* cells (Fischer et al., 2015). Pairwise knockdown combinations (2 × 2 dsRNAs) were used to detect and avoid off-target effects. The study comprised 1,367 *Drosophila* genes implicated in different cellular processes, including signaling, chromatin, and cell-cycle regulation, and scored 21 phenotypes in cultured cells. The multi-parametric phenotypes allow researchers to infer protein function and clustered processes on the basis of similarity. Using multiple phenotypes also facilitates computation of directional genetic interactions and maps for logical or temporal dependencies between genes. Similar approaches have also been feasible in mammalian cells (Laufer et al., 2013; Roguev et al., 2013; Wang et al., 2014)

High-content imaging has also been combined with other methods to measure whole-proteome dynamics under different environmental conditions (Chong et al., 2015). GFP-fusion proteins were used in yeast to map localization for more than 3,000 proteins with high-throughput, confocal microscopy in single cells. Protein localization classifiers that were derived through machine learning using image-derived features from previously established protein localization have been applied to the whole dataset. This approach has been used to determine proteome-wide abundance as well as relocalization of proteins after treatment with several drugs.

Perturbation Reagents

In most cases, cell-based assays use small-molecule or RNAi libraries as perturbation reagents. Perturbation reagent libraries can contain many thousands of reagents in micro-well plate formats. High-content screens are typically incompatible with "pooled" screening formats using retroviral or lentiviral delivery of complex short-hairpin or short-guide RNA libraries. In such screens, cells are transfected in bulk, and perturbations are identified through selection and subsequent isolation as well as sequencing of the enriched or depleted silencing reagent (Moffat et al., 2006; Shalem et al., 2015). Although certain cell-based assay parameters differ between RNAi and small compound screens (such as incubation time and use of transfection reagents), similar assays have been used for different perturbation assays (Eggert et al., 2004; Sundaramurthy et al., 2013). Figure 2 shows typical workflows for image-based high-throughput screens.

RNAi Libraries

Imaged-based experiments require RNAi in an arrayed format. Currently, most image-based screens use siRNA, enzymatically prepared (esi) RNA (in humans or mice) (Kittler et al., 2004, 2007), or long double-stranded (ds) RNA (*Drosophila*) (Horn et al., 2010; Ramadan et al., 2007). Genome-scale RNAi reagent libraries are available from different academic and commercial sources. For many organisms, in addition to genome-wide libraries, sub-libraries for specific functional groups, e.g., all kinases and surface proteins, have been generated, thus facilitating focused, high-content screening experiments. Off-target effects are a major concern for all RNAi experiments (Echeverri et al., 2006). In certain cases, libraries proceeded through several iterations to limit off-target effects from RNAi reagents as much as possible (Horn et al., 2010; Mohr et al., 2010) using multiple, sequence-independent reagents. Concordant multi-parametric phenotypes have been used to predict specific reagents (Horn et al., 2011).

Small-Molecule Libraries

Depending on the focus and size of the experiment, various small-molecule libraries, available from commercial or academic sources, may be used. Academic screening centers have been established at multiple locations to facilitate access to libraries, small-molecule screening expertise, and chemistry follow-up. Recently, several public-private partnerships have been established to provide access to a large collection of small molecules (Mullard, 2013; Roy et al., 2010).

Experimental Design: General Considerations

Image-based assays and establishing conditions for subsequent high-throughput screens often require multiple iterations of protocol optimization. Many questions must be initially addressed, including the following: What type of cells should be used? What is the intended size of the screen? What are suitable

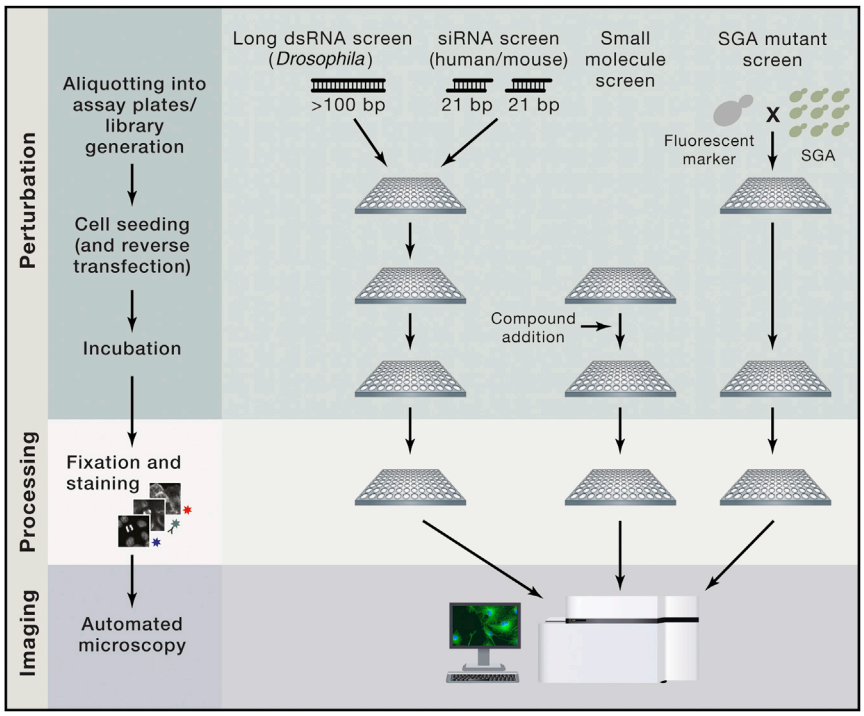

Figure 2. Workflows of Image-Based Screens using Different Perturbation Reagents

Despite differences in perturbation agent, cellular model, or experimental scope, the main steps of an image-based screen are similar. The library of perturbation reagents is distributed onto assay plates, then cells are seeded into the wells (and, if applicable, reversely transfected with RNAi reagents). In microscopy screens in yeast, fluorescently tagged reporters can be crossed into library mutant strains. Following an incubation time of typically 24 to 96 hr, the cells are fixed and stained with fluorescent probes that label the relevant cellular features. Subsequently, the images are captured by automated microscopy and passed on to the image-analysis pipeline. SGA: synthetic genetic arrays.

perturbation reagents? How complex should the phenotypic read-out be? Furthermore, conducting large-scale imaging screens differs in many aspects from conducting smaller-scale experiments. Establishing and scaling a high-content screening assay often requires several months, but the screen is often performed in a short time frame, depending on the size of the library. It is also important that the establishment of the experimental assay and image-analysis workflows are tightly linked (Figure 3). The following section describes general considerations that are important in high-content screens.

Imaged-based screens can be performed in high-density cell culture plates with 96, 384, or 1,536 wells; 384-well plates are the most frequently used assay format. Alternatively, reagents such as small molecules and siRNA have also been spotted onto microscopy slides (Neumann et al., 2006; Wheeler et al., 2004). The set of genes to be screened is determined by the scientific question and—together with the phenotypic read-out complexity—defines the experimental scale. The size of the experimental set must sometimes be reduced for compatibility with high-resolution or confocal imaging experiments. A frequently used approach includes screening defined functional groups, such as kinases or phosphatases. Another strategy has been to first identify candidate genes through a genome-wide screen and then perform a secondary screen with a more complex phenotypic analysis. For example, Simpson et al. (2012) followed this strategy when they first screened genome-wide siRNAs for secretion regulators through assaying transport of fluorescently labeled tsO45G to the plasma membrane, and ~500 genes that inhibited secretion were identified. In a secondary screen, these candidates were further analyzed in more complex secondary assays using fluorescence labeling of COPI and COPII coats as well as the Golgi matrix protein GM130 (Simpson et al., 2012).

Positive and negative controls must be added to each plate to assess assay reproducibility and normalize potential batch effects. Fluorescent probes and/or genetically encoded fluorescent proteins must be selected and validated in smaller-scale experiments. Another important factor to consider is the experimental time span because, for example, this determines the number of cells that can be seeded in high-density tissue culture plates. Often, small-molecule screens use short incubation times (24–48 hr), whereas RNAi screens typically require 72 hr or a longer incubation time to ensure target protein depletion. The experimental design should also implement built-in quality controls, including plate designs that assign a sufficient number of wells for the controls. For RNAi screens, it is preferable to arrange reagents in a random order. Some commercially available RNAi libraries are sorted by gene name, which can produce normalization problems during data-analysis steps due to overrepresentation of related genes on the same assay plate.

A crucial aspect of the assay design phase is assessing and optimizing experimental reproducibility. Technical variations must be reduced, error-prone pipetting steps must be limited, and variation between the reagent or consumable lots must be avoided. This aspect can be implemented, in part, through automating pipetting steps by using liquid-handling robots to prepare screening plates and seed cells as well as for staining procedures.

Steps in Performing Image-Based Screens

Despite differences in assay setup, experimental scale, or phenotypic read-out, certain general steps are necessary for performing an image-based screen. The overall scientific question addressed by the high-throughput experiment often dictates the cell type used and the phenotype scored. Additionally, many parameters are interdependent; for example, the cell type determines transfection protocol and experimental timescale. An imaging assay also comprises cell fixation, staining, and microscopy, which must be adapted for the screen. Image-analysis

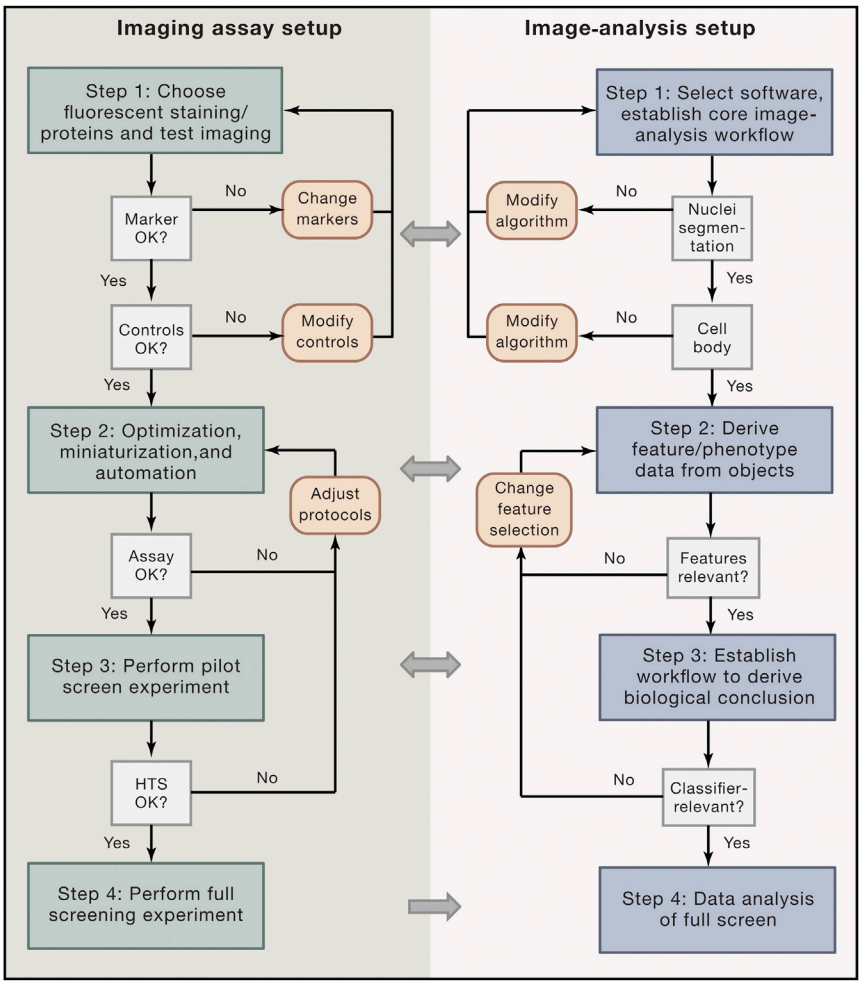

Figure 3. Workflow and Decision Tree for Assay Development and Image Analysis

The development of a high-throughput image-based assays and image-analysis procedures should ideally be done in parallel.

Step 1: Staining procedures are established at a small scale. Selected probes should specifically stain the structures of interest without generating a strong unspecific background; exposure times need to be optimized. Alternative stains need to be tested if markers are not suitable (Marker OK?). The staining should be tested on positive and negative controls to ensure that the expected phenotypes are depicted (Controls OK?). In parallel, a basic image-analysis pipeline should be established. The algorithms have to be modified until nuclei and cell bodies (or subcellular structures) are segmented correctly. Staining procedures have to be modified, if necessary.

Step 2: The assay is miniaturized for high-throughput and automated to ensure high reproducibility. Handling of cells is established, and the adequate number of cells seeded is tested. If possible, the protocol steps should be minimized; individual steps can be combined. In parallel, the image analysis is optimized. The quantitative features extracted by the software must reflect relevant phenotypes (Features relevant?). If necessary, the feature selection must be changed. Also, technical and biological reproducibility is tested, and quality-control measures as well as data normalization are established.

Step 3: The assay is subjected to realistic screening conditions in a pilot screen. Critical points such as cell survival, batch processing, timing, and automation need to function at high-throughput (HTS OK?). Image quality, software performance, computational power, and data handling and storage are assessed. Finally, a data-analysis workflow to extract biological information from the gained phenotypic features is set up and tested (Classifier relevant?).

Step 4: Full screening experiment and data analysis.

steps should be implemented in parallel because this procedure provides direct feedback on the suitability of the assay. Figure 3 provides an overview of the different assay development steps and their interconnections. Below, we describe certain key parameters for constructing high-content screening experiments and use examples to illustrate the parameters.

Cell Model

The cell line must be selected when assay development begins. The cell model should be relevant to the questions to be addressed and suitable for large-scale screens. Many established cell lines perform well in large-scale experiments, but cell characteristics might change over time and may not reflect the original biological context. Primary cells, however, often retain the specific physiological characteristics of their tissue source or disease context but are often difficult to expand and require more careful handling during the experiment. In addition, perturbation experiments are often more difficult to perform when using primary cells.

For example, Nieland et al. (2014) have screened for genes required in synapse formation. To perform the screen in primary cells, they established generation and culture conditions for mouse primary cortical neurons and developed an image-analysis process to capture synaptogenesis through fluorescently labeling four process-related proteins. Due to limitations in throughput, they screened 116 selected mouse genes using a lentiviral shRNA library and described several novel putative positive regulators of synapse formation (Nieland et al., 2014). In another example, Sepp et al. (2008) were interested in primary neuron morphological phenotypes. Using fluorescently labeled *Drosophila* primary neurons, they performed a genome-wide screen with an imaging read-out and identified 104 conserved genes involved in neurite outgrowth (Sepp et al., 2008).

Other experiments might require a defined mutational status to analyze a signaling pathway or expression of specific proteins or to introduce disease-related mutations. For example, Honarnejad et al. (2013) sought to elucidate the mechanisms involved in impaired calcium homeostasis associated with presenilin-1 mutations, which is linked to familial Alzheimer's disease. They introduced a presenilin-1 mutant into HEK293 cells and screened 20,000 small molecules for reversal of the induced calcium alterations. Their screen produced 52 primary hits and led to the identification of 4 candidates (Honarnejad et al., 2013).

Fluorescent Probes

To visualize phenotypes, most high-content screens use fluorescent probes for staining or to genetically encode fluorescent proteins. Fluorescent read-outs can differ; therefore, certain general considerations apply. The simplest phenotype, e.g., number of cells after perturbation, can be determined from low-resolution images after DNA staining. In many cases, the imaging read-out will be more complex with multiple fluorescent channels, confocal microscopy, and/or live-cell imaging.

Many antibodies and fluorescent probes are available for staining cellular features, such as a cell membrane, DNA or organelles, and certain proteins. A probe should specifically stain the structure of interest without much background, which might impede image analyses. Additionally, the fluorescent stain should be sufficiently bright to allow for short exposure times, thereby decreasing image-acquisition time. When combining multiple fluorescent probes, it is important to avoid bleed-through between channels. In general, researchers should use only as many probes or antibodies as necessary to avoid prolonging the imaging time. In the first step, the probe should be tested on a small scale to confirm suitability for the planned assay. Subsequently, the probe should be tested on positive and negative controls to ensure that the key phenotypes are measurable.

Miniaturization and Automation

In a second step, the assay must be miniaturized and adapted for high-throughput settings. Often, this step involves automating the screening procedure, including cell-seeding and pipetting steps during fixation and staining (Laufer et al., 2014). Miniaturizing the imaging read-out to a 96- or 384-well format is desirable because seeding and growing cells must be established in a small volume. These optimization steps must address a number of different experimental questions, such as the following: Do the cells survive mass preparation and automated liquid handling? Do they grow to the desired density to ensure sufficient cells for analysis? Do they overgrow in the well, impeding proper cell segmentation by the analysis software? Moreover, the fluorescence-staining procedures must be robust and suitable for automation; for example, they should require as few pipetting steps as possible. Fluorescently labeled antibodies may be preferable over primary and secondary antibody combinations. Miniaturization and automation might also support combined processing steps; for example, fixation and permeabilization might be performed together, or all staining steps might be performed in parallel.

Once a screening protocol is established, a pilot screen can be performed on a smaller gene set to evaluate performance of the assay protocol under high-throughput conditions. Miniaturization and automation of experiments can reveal unexpected sources of problems that need to be solved before the full-scale screen. A pilot screen also serves as a proof of concept, demonstrating that the experimental design is suitable for screening at a larger scale. Neumann et al. (2006) developed an automated high-throughput approach for RNAi screening using time-lapse imaging of a HeLa cell line stably expressing GFP-tagged His2B (Neumann et al., 2006). In a pilot screen, they perturbed 49 genes by RNAi, demonstrating that the assay is suitable for a genome-wide cell-cycle experiment (Neumann et al., 2010).

Image Acquisition

Image acquisition is a crucial step for high-content screening because the image quality determines the overall screen quality. In this step, the image resolution and magnification must be defined to capture the required details for the phenotype but provide sufficient cell counts for robust statistics. When high magnification is necessary, such as to analyze subcellular structures, several images per well may be required to capture a sufficient number of cells. Exposure time is another critical factor that must be adapted for each fluorescence channel. Most automated microscopes have an autofocus option based either on a hardware or software method. Exposure time and focus are two variables that require multiple optimization iterations and may require adaptation prior to imaging experiments. Care must be taken to avoid imaging artifacts, such as uneven illumination or a decaying light source during a high-content screening experiment. Data handling and storage protocols should also be established in parallel with assay development. Large-scale imaging screens can easily produce several terabytes in one experiment. A combinatorial RNAi screen performed in our lab to measure genetic interactions produced roughly 5.6 terabytes of imaging data from 160 384-well plates (Laufer et al., 2013).

Image Analysis: From Images to Phenotypes

To deduce biological information from an image-based screen, numeric measurements must be extracted and processed. "Computer vision" methodologies determine descriptors (features) that summarize the information encoded by spatially resolved pixel-intensity patterns (Danuser, 2011). The most suitable descriptors for implementing an analysis workflow depend on the marker type used for imaging. Implementing image-analysis pipelines in parallel to optimizing the screening workflow is preferred (Figure 3). In the following paragraphs, we review basic analysis methods and describe how they can be applied for the analysis of high-content screening data.

In high-content screening, phenotypes are defined as a complex description of the cellular or organismal response toward an experimental perturbation. In certain cases, phenotypes have clear cell-biological correlates, such as large cells, mitotic cells, and apoptotic bodies, but phenotypes can also be subtle changes in the distribution of fluorescent markers. Computationally, a phenotype is a vector of numeric features derived from the analyzed image. These features are calculated for a *region of interest* (ROI, e.g., individual cells or nuclei) or the entire image. Identifying ROIs through computer-vision algorithms is referred to as segmentation.

Image analysis can be roughly divided into two major analytic steps. The first step includes image processing, object or ROI identification, and feature extraction. This step is typically performed with specialized image-analysis software such as CellProfiler (Carpenter et al., 2006), EBImage (Pau et al., 2010), or ImageJ/Fiji (Schindelin et al., 2012) (Table 1). These software packages each have different advantages and disadvantages, such as analysis speed or an intuitive user interface, but they all perform most image-processing steps. The size of high-throughput datasets can pose significant challenges for image data processing; therefore, many image-analysis software

Table 1. Open-Source Image-Analysis Software

Name	Type	Website	Reference	Description
CellCognition	time-lapse image analysis	http://www.cellcognition.org/	(Held et al., 2010)	CellCognition is a cross-platform image-analysis software for the analysis of time-lapse experiments.
CellProfiler	low- to high-throughput image analysis	http://www.cellprofiler.org	(Carpenter et al., 2006)	Modular open-source software with intuitive user interface.
CellProfiler Analyst	machine-learning cell classification	http://www.cellprofiler.org/	(Jones et al., 2008)	CellProfiler Analyst is an open-source software for exploring and analyzing large, high-dimensional image-derived data.
EBImage	low- to high-throughput image analysis, machine-learning cell classification	http://www.bioconductor.org/packages/release/bioc/html/EBImage.html	(Pau et al., 2010)	EBImage is an R package that provides general purpose functionality for the reading, writing, processing, and analysis of images.
Fiji/ImageJ	general purpose image-analysis software framework	http://fiji.sc/	(Schindelin et al., 2012)	Fiji is a distribution of ImageJ for the life sciences.

packages facilitate distributed image processing on multi-CPU clusters to decrease screening-experiment analysis times.

Image Data

The input data for computer-vision algorithms are images or stacks of images, depending on the image-acquisition mode. For high-content screens, the most commonly used approach is multi-channel fluorescence microscopy. Depending on the specimen size, these images can also resemble mosaics of neighboring ROIs (e.g., tiles of a micro-well). Depending on the microscopy camera detector, images feature different resolutions (pixel dimensions) that currently range from 512 × 512 to 2,048 × 2,048 pixels with up to 65,536 different intensities. Spatial or intensity binning can reduce image size; however, this procedure results in loss/blurring, which might interfere with image-analysis steps. A high-content experiment can yield hundreds of thousands of images. For example, a screen comprising 100 384-well plates imaged with three fluorescent channels at four independent sites per well produces 460,800 images. As more dimensions are added to the experiment, such as in time-lapse studies or for additional fluorescence channels or confocal z stacks, storage capacity and computational infrastructure for data handling might become a limiting factor.

Image Processing and Segmentation

First, images are imported, cropped to an equal size, registered, and corrected for noise and illumination errors (Wang, 2007). Noise can have different origins, such as random photon emission from the background ("salt-and-pepper noise"), staining artifacts, dirt speckles, or optic aberrations, such as laser beam convolution. Often, noise can be corrected by applying different types of filters, which all use kernel-based methods for image smoothing (Wang, 2007). These filters can be linear, such as mean, median, or Gaussian filters, or non-linear, such as the Canny-edge filter (Rank and Unbehauen, 1992). After image filtering, images with normalized and smoothened intensity histograms can be passed to the next step of binarization. In this step, each pixel is assigned to either the foreground or background. Binarization can be performed by applying either histogram-based methods of dichotomization, such as Otsu's threshold, or local pixel neighborhood-dependent methods, such as local adaptive threshold (Otsu, 1979). For cell segmentation, the most commonly used method is to tag each region of connected pixels in the binarized DNA channel as the nucleus.

Cell-body segmentation is often performed by Voronoi tessellation-based methods, but also other methods, such as balloon-growing algorithms (Beneš and Zitová, 2015), can be used. Each ROI identified resembles one stained cell, and its outlines can be used to control the segmentation process. For many cases, this process is precise; however, several pitfalls must be considered. Constructing a segmentation pipeline for one particular image is often straightforward; however, the same pipeline might over-segment or under-segment different images in a large-scale dataset. Typically, in under-segmented images, "real" objects are not detected, but over-segmentation leads to detection of background noise or other unrelated objects (Thompson et al., 2014), and, thus, objects may be artificially combined or split into several objects. Under screening conditions, this is especially challenging because unexpected phenotypes might not be captured by the test set used to optimize the analysis. Thus, the pipelines should be optimized on a large and diverse set of test images, such as those obtained through pilot screening experiments. Ensuring sufficient quality of the segmentation analysis is particularly important in large-scale screens because segmentation quality is impossible to manually control for hundreds of thousands of samples.

Extracting Numerical Features

Once objects are defined by the segmentation pipeline, numeric features are extracted and quantitatively describe these regions. Generic features, which can be extracted from objects in fluorescence images, can be separated into four categories: (1) marker-intensity features that describe the pixel-intensity statistics of a certain channel inside the outline of the ROI; (2)

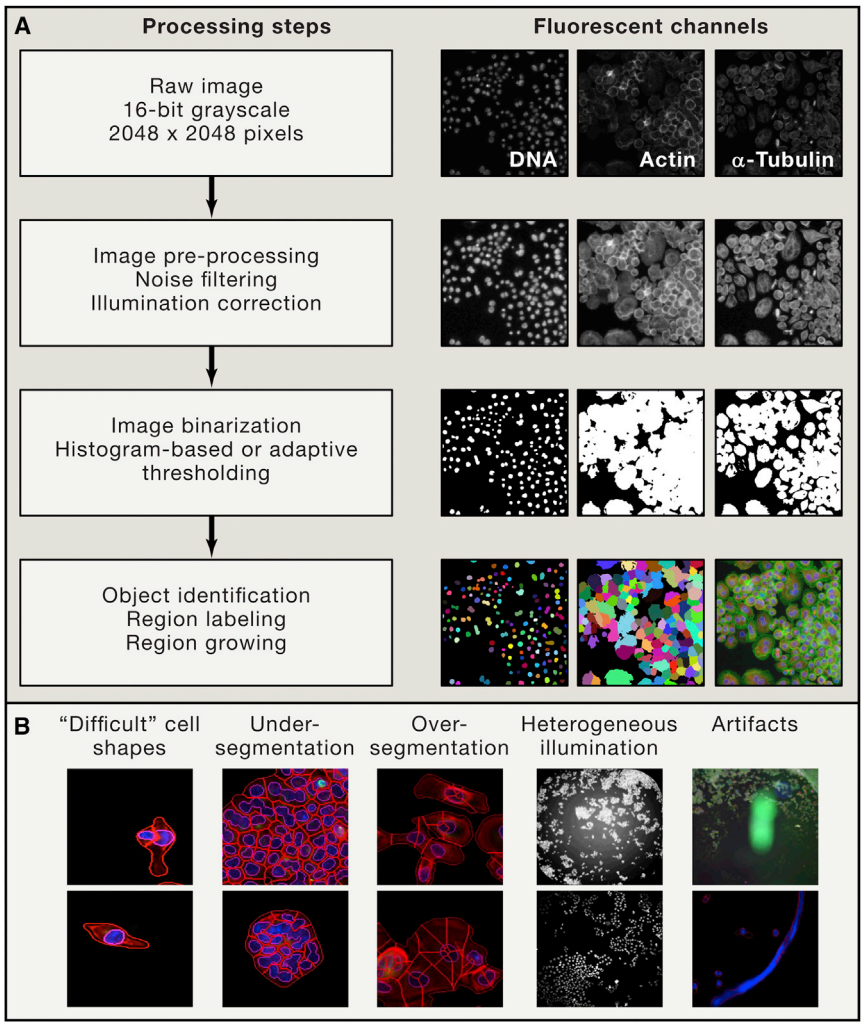

Figure 4. Image Analysis

Most image-processing pipelines follow the same principal steps exemplified here.

(A) Images of *Drosophila* cells stained with fluorescent markers for DNA, actin, and tubulin. First, for object recognition, images need to be corrected for stochastic and systematic errors, such as salt-and-pepper noise, emission convolution, or un-even specimen illumination patterns. Second, all channels are binarized whereby each pixel based on its properties or the properties of its neighborhoods is assigned to either fore- or background. After binarization, objects are defined as connected areas of pixels. In case nuclei and bodies should be segmented together, objects are labeled in the DNA channel and expanded into the binary body-objects mask by propagation of their outlines.

(B) Image artifacts can hinder image analysis: artifacts can originate, e.g., from the image acquisition (illumination patterns, air bubbles, or dirt) or sub-optimal image segmentation (such as under- or over-segmentation).

object-shape features that describe the geometric features of each segmented object, such as its size or roundness; (3) moment features that describe the spatial situation of objects in the image, such as the direction of the major axis or center of mass; and (4) texture features that describe the distribution of pixel-intensity values throughout the ROI. Texture features were first proposed by Haralick and Zernike and describe how neighboring pixels inside an ROI interact, co-occur, or distribute. In a recent study (Liberali et al., 2014), 200 features from each single cell in high-content screens were extracted and used to train a support vector machine based on supervised cell classification. Segmentation of 2 × 10^6 images was based on DAPI and CellTrace staining and analyzed using CellProfiler (Liberali et al., 2014).

Feature Reduction

Although several hundred features can be extracted from each ROI, the features are often generic, and the connection to biologically interpretable phenotypes is unclear. As a next step, different procedures can be used to reduce the number of features, such as through selecting the features that provide non-redundant information using stepwise selection algorithms (Fischer et al., 2015). Alternatively, manual annotation or supervised or unsupervised machine learning may be used to select informative features (Held et al., 2010; Sommer and Gerlich, 2013). These phenotypes often reflect broader biological characteristics and combine various generic features (Fischer et al., 2015; Fuchs et al., 2010; Neumann et al., 2010). Feature reduction also aids in focusing on the most meaningful features and removes unnecessary data (Figures 5B and 5C). For example, in many assays, the exact X-Y location of each cell in the well is typically not linked to a biological process triggered by a particular perturbation and is discarded (Fischer et al., 2015; Horn et al., 2011).

Image Analysis: How to Derive Biological Meaning

Phenotypic similarities can be used to cluster genes into functionally related groups on the basis of the assumption that perturbations triggering the same biological process will produce a similar phenotype. Different methods can be used to classify phenotypes: (1) Methods apply supervised clustering, whereby classifiers are trained on a manually curated dataset of "known" phenotypes. These classifiers are then applied to the full dataset to categorize the perturbations. Such an analysis has been performed, for example, in Fuchs et al. (2010) and Neumann et al. (2010) for RNAi screens and in Loo et al. (2007) and Eggert et al. (2004) for small-molecule screens (Eggert et al., 2004; Fuchs et al., 2010; Loo et al., 2007; Neumann et al., 2010) (Figure 5D). (2) Unsupervised methods, such as k-means or hierarchical clustering, avoid restrictions imposed by the training dataset. These methods are suitable for discovery of new unexpected phenotypes in a dataset or when little is known about the dataset

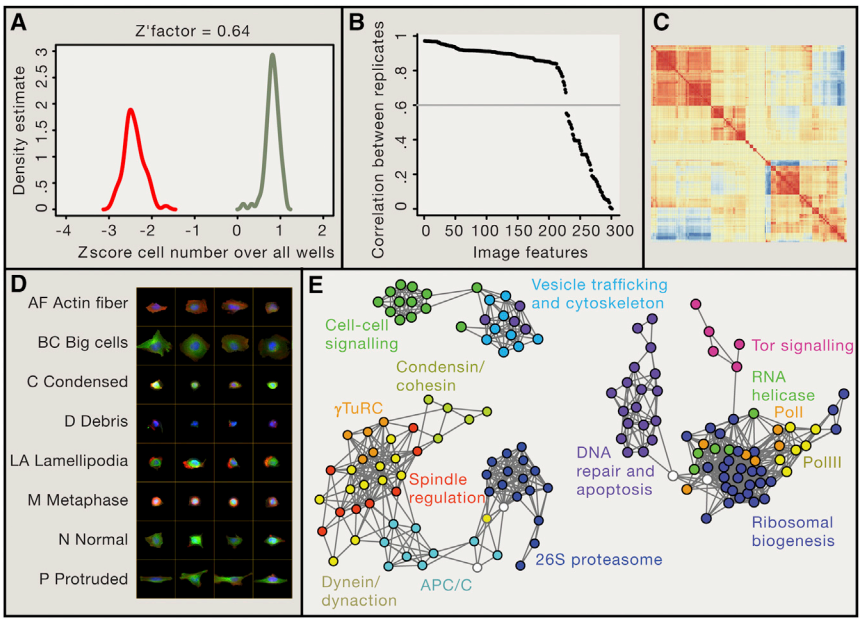

Figure 5. Data Analysis

Data from image-based screens are analyzed by a multi-step process.

(A) Quality-control plots to assess stability of assays. Positive and negative control distributions should be well separated. Z' factors are a measure of assay performance as described in Zhang et al. (1999). A Z' factor > 0.5 indicates a very good assay performance.

(B) Correlation of features between biological replicates can be used to exclude features that are not very reproducible.

(C) Correlation between features can reveal redundant features. Clustering of features with high correlations identify potentially redundant features.

(D) Features can be summarized by supervised or unsupervised classification into phenotypic classes. Shown are images of cells classified by a supervised classification approach (Fuchs et al., 2010).

(E) Genes or genetic interaction can be clustered according to their feature vectors. A graph of genes derived from a multi-parametric gene-gene interaction experiments is shown (Fischer et al., 2015).

(Horn et al., 2011; Nir et al., 2010; Yin et al., 2013). Multi-variate phenotype data can be visualized in many ways, such as clustered network graphs, clustered heat maps, or phenotype representations (Figure 5E). Specific graphical visualization methods have been developed to display phenotypes and map features onto abstract images of cells (Sailem et al., 2015), which is useful for representing the biological meaning of features.

Quality control of image-analysis pipelines is performed on multiple levels. The overall quality of images greatly impacts the analysis results. Therefore, continuous efforts have to be undertaken in screens to avoid or exclude artifacts. In large-scale screens, quality of the images can be impacted by illumination problems, dust, and other particles that need to be recognized and excluded by the analysis workflow. Examples of problems that occur in high-content screens are plentiful (examples are shown in Figure 4B). After the analysis steps, the biological relevance of the extracted data can be assessed on internal control perturbations for which the cellular response is known. The performance of control perturbations included in the screening experiment also enables assessment of the quality of the experimental and computational workflows (see also Figure 5A).

Novel Assays and Screening Approaches

Currently, most high-content screens rely on antibody staining for the proteins of interest or overexpression of fluorescently tagged proteins or dyes. With new technologies to re-engineer a cell's genome, genetic modifications for new assays that were previously feasible only in ESCs may soon be readily performed in many cell types. In particular, it is now feasible in almost all cell lines to create endogenously tagged fluorescent proteins by homologous recombination using CRISPR/Cas9-mediated genome engineering (Figure 6) (Kimura et al., 2015). By identifying suitable short-guide (sg) RNA sites using different available software tools (Heigwer et al., 2014; Montague et al., 2014), donor templates can be used to recombine in-frame fluorescent fusion proteins (Ran et al., 2013). This approach avoids overexpressing tagged proteins or using BAC constructs and might also facilitate use of multiple tagged proteins with different fluorescent colors.

Instead of using artificial reporter constructs, CRISPR/Cas9-mediated engineering will also facilitate generation of reporter cell lines expressing fluorescent proteins that are controlled by endogenous promotor and enhancer sequences. Such approaches have been broadly used in ESCs and in vivo and have provided important insights into spatial and dynamic control of cellular pathways (Lauschke et al., 2013); however, the approaches have been difficult to implement for screening assays in most commonly used cell lines. These approaches are also suitable for combining different colors, which should facilitate assays that exceed currently available methodologies. Creating multiplex assays will also become technically feasible. For example, multiple components and transcriptional targets can be assessed in parallel without further complex staining procedures that are currently used in high-content screening (Figure 6C). Novel methodologies that create sensitive, endogenous probes could further enhance assay performance (Tanenbaum et al., 2014).

Another area of active development is improvement and accessibility of image-analysis workflows to enhance multi-parametric phenotype analyses. A recent survey has reported that most published high-content screens are not multi-parametric and only partially make use of the richness of the image data (Singh et al., 2014). Increasing information from image-based screens by making software workflows more easily accessible remains an important goal.

Outlook and Concluding Remarks

During the past years, methods to automatically derive phenotypes from image-based screens have matured and enabled

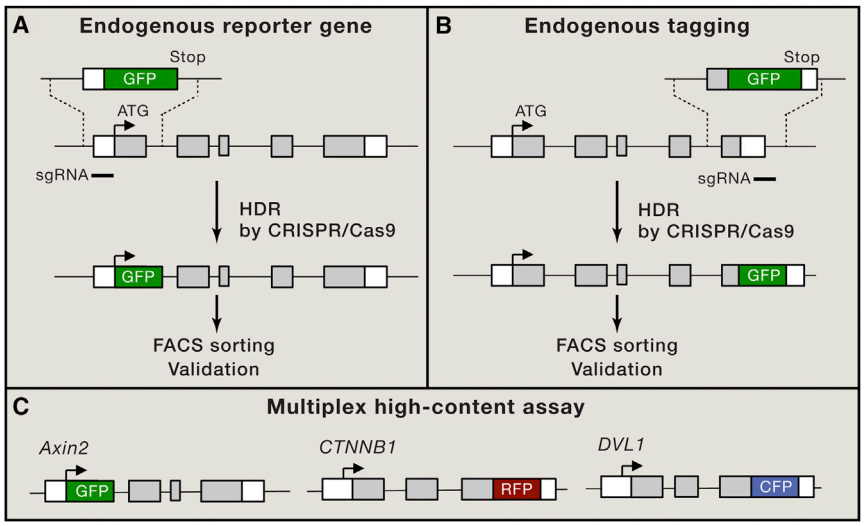

Figure 6. Novel Assays for High-Content Screens

Schematic description on how to generate endogenously tagged genes by CRISPR/Cas9-mediated genome engineering.

(A) Endogenous reporter genes for image-based screens can be generated by recombineering of fluorescent proteins behind the start codon. A stop cassette terminates the gene after the fluorescent protein.

(B) Alternatively, proteins could be tagged to monitor changes in localization or stability as indicators for specific cellular processes.

(C) Genome engineering would also allow combination of multiple reporter/tagging approaches to create multiplex assays that monitor signaling pathway activity at multiple levels. HDR: homologous directed repair. RFP: red fluorescent protein. CFP: cyan fluorescent protein.

the application of high-content screening methods to many biomedical questions. With the availability of additional perturbation reagents and new developments in assay technologies, it can be expected that visual, multi-parametric screening approaches will continue to advance the systematic understanding of cellular processes. Nevertheless, there are a number of challenges on both the experimental as well as computational side that will need further developments, including higher-resolution microscopes and novel imaging modalities.

Currently, most screens have been performed on a limited number of cell lines for which protocols for high-throughput screening are readily available. For many biological assays the question about the most relevant cell system remains often unresolved. In the future, isogenic cell-line models and induced pluripotent cells (iPSCs) might enable the generation of more specific cell models for basic as well as disease-relevant questions. Large collections of cell lines with defined genotypes have previously been used to determine drug sensitivity using cell growth and viability as a phenotypic read-out. Increasing the complexity of the phenotypic read-out beyond lethality could enable a deeper understanding of drug-gene relationships. In addition, 3D cell models, such as organoids, might be adapted for high-content screening experiments. Primary cell models could also be used for phenotyping cells with complex genetic backgrounds (Dermitzakis, 2012) and enable the use of image-based phenotypes to dissect cellular correlates of complex traits.

ACKNOWLEDGMENTS

We thank members of the Boutros lab for helpful comments on the manuscript. Research in the lab of M.B. is supported by an ERC Advanced Grant ("Syngene") from the European Commission.

REFERENCES

Beneš, M., and Zitová, B. (2015). Performance evaluation of image segmentation algorithms on microscopic image data. J. Microsc. *257*, 65–85.

Bier, E. (2005). Drosophila, the golden bug, emerges as a tool for human genetics. Nat. Rev. Genet. *6*, 9–23.

Björklund, M., Taipale, M., Varjosalo, M., Saharinen, J., Lahdenperä, J., and Taipale, J. (2006). Identification of pathways regulating cell size and cell-cycle progression by RNAi. Nature *439*, 1009–1013.

Boutros, M., and Ahringer, J. (2008). The art and design of genetic screens: RNA interference. Nat. Rev. Genet. *9*, 554–566.

Boutros, M., Kiger, A.A., Armknecht, S., Kerr, K., Hild, M., Koch, B., Haas, S.A., Paro, R., and Perrimon, N.; Heidelberg Fly Array Consortium (2004). Genome-wide RNAi analysis of growth and viability in Drosophila cells. Science *303*, 832–835.

Carpenter, A.E. (2007). Image-based chemical screening. Nat. Chem. Biol. *3*, 461–465.

Carpenter, A.E., Jones, T.R., Lamprecht, M.R., Clarke, C., Kang, I.H., Friman, O., Guertin, D.A., Chang, J.H., Lindquist, R.A., Moffat, J., et al. (2006). CellProfiler: image analysis software for identifying and quantifying cell phenotypes. Genome Biol. *7*, R100.

Chia, N.-Y., Chan, Y.-S., Feng, B., Lu, X., Orlov, Y.L., Moreau, D., Kumar, P., Yang, L., Jiang, J., Lau, M.-S., et al. (2010). A genome-wide RNAi screen reveals determinants of human embryonic stem cell identity. Nature *468*, 316–320.

Chong, Y.T., Koh, J.L.Y., Friesen, H., Duffy, S.K., Cox, M.J., Moses, A., Moffat, J., Boone, C., and Andrews, B.J. (2015). Yeast proteome dynamics from single cell imaging and automated analysis. Cell *161*, 1413–1424.

Danuser, G. (2011). Computer vision in cell biology. Cell *147*, 973–978.

Dermitzakis, E.T. (2012). Cellular genomics for complex traits. Nat. Rev. Genet. *13*, 215–220.

Desbordes, S.C., and Studer, L. (2013). Adapting human pluripotent stem cells to high-throughput and high-content screening. Nat. Protoc. *8*, 111–130.

Desbordes, S.C., Placantonakis, D.G., Ciro, A., Socci, N.D., Lee, G., Djaballah, H., and Studer, L. (2008). High-throughput screening assay for the identification of compounds regulating self-renewal and differentiation in human embryonic stem cells. Cell Stem Cell *2*, 602–612.

Echeverri, C.J., Beachy, P.A., Baum, B., Boutros, M., Buchholz, F., Chanda, S.K., Downward, J., Ellenberg, J., Fraser, A.G., Hacohen, N., et al. (2006). Minimizing the risk of reporting false positives in large-scale RNAi screens. Nat. Methods *3*, 777–779.

Eggert, U.S., Kiger, A.A., Richter, C., Perlman, Z.E., Perrimon, N., Mitchison, T.J., and Field, C.M. (2004). Parallel chemical genetic and genome-wide RNAi screens identify cytokinesis inhibitors and targets. PLoS Biol. *2*, e379.

Eliceiri, K.W., Berthold, M.R., Goldberg, I.G., Ibáñez, L., Manjunath, B.S., Martone, M.E., Murphy, R.F., Peng, H., Plant, A.L., Roysam, B., et al. (2012). Biological imaging software tools. Nat. Methods *9*, 697–710.

Fischer, B., Sandmann, T., Horn, T., Billmann, M., Chaudhary, V., Huber, W., and Boutros, M. (2015). A map of directional genetic interactions in a metazoan cell. eLife *4*, 4.

Fuchs, F., Pau, G., Kranz, D., Sklyar, O., Budjan, C., Steinbrink, S., Horn, T., Pedal, A., Huber, W., and Boutros, M. (2010). Clustering phenotype populations by genome-wide RNAi and multiparametric imaging. Mol. Syst. Biol. *6*, 370.

Heigwer, F., Kerr, G., and Boutros, M. (2014). E-CRISP: fast CRISPR target site identification. Nat. Methods *11*, 122–123.

Held, M., Schmitz, M.H.A., Fischer, B., Walter, T., Neumann, B., Olma, M.H., Peter, M., Ellenberg, J., and Gerlich, D.W. (2010). CellCognition: time-resolved phenotype annotation in high-throughput live cell imaging. Nat. Methods *7*, 747–754.

Honarnejad, K., Daschner, A., Giese, A., Zall, A., Schmidt, B., Szybinska, A., Kuznicki, J., and Herms, J. (2013). Development and implementation of a high-throughput compound screening assay for targeting disrupted ER calcium homeostasis in Alzheimer's disease. PLoS ONE *8*, e80645.

Horn, T., Sandmann, T., and Boutros, M. (2010). Design and evaluation of genome-wide libraries for RNA interference screens. Genome Biol. *11*, R61.

Horn, T., Sandmann, T., Fischer, B., Axelsson, E., Huber, W., and Boutros, M. (2011). Mapping of signaling networks through synthetic genetic interaction analysis by RNAi. Nat. Methods *8*, 341–346.

Jones, T.R., Kang, I.H., Wheeler, D.B., Lindquist, R.A., Papallo, A., Sabatini, D.M., Golland, P., and Carpenter, A.E. (2008). CellProfiler Analyst: data exploration and analysis software for complex image-based screens. BMC Bioinformatics *9*, 482.

Karim, F.D., Chang, H.C., Therrien, M., Wassarman, D.A., Laverty, T., and Rubin, G.M. (1996). A screen for genes that function downstream of Ras1 during Drosophila eye development. Genetics *143*, 315–329.

Karlas, A., Machuy, N., Shin, Y., Pleissner, K.-P., Artarini, A., Heuer, D., Becker, D., Khalil, H., Ogilvie, L.A., Hess, S., et al. (2010). Genome-wide RNAi screen identifies human host factors crucial for influenza virus replication. Nature *463*, 818–822.

Kiger, A.A., Baum, B., Jones, S., Jones, M.R., Coulson, A., Echeverri, C., and Perrimon, N. (2003). A functional genomic analysis of cell morphology using RNA interference. J. Biol. *2*, 27.

Kimura, Y., Oda, M., Nakatani, T., Sekita, Y., Monfort, A., Wutz, A., Mochizuki, H., and Nakano, T. (2015). CRISPR/Cas9-mediated reporter knock-in in mouse haploid embryonic stem cells. Sci Rep *5*, 10710.

Kittler, R., Putz, G., Pelletier, L., Poser, I., Heninger, A.K., Drechsel, D., Fischer, S., Konstantinova, I., Habermann, B., Grabner, H., et al. (2004). An endoribonuclease-prepared siRNA screen in human cells identifies genes essential for cell division. Nature *432*, 1036–1040.

Kittler, R., Surendranath, V., Heninger, A.-K., Slabicki, M., Theis, M., Putz, G., Franke, K., Caldarelli, A., Grabner, H., Kozak, K., et al. (2007). Genome-wide resources of endoribonuclease-prepared short interfering RNAs for specific loss-of-function studies. Nat. Methods *4*, 337–344.

Laufer, C., Fischer, B., Billmann, M., Huber, W., and Boutros, M. (2013). Mapping genetic interactions in human cancer cells with RNAi and multiparametric phenotyping. Nat. Methods *10*, 427–431.

Laufer, C., Fischer, B., Huber, W., and Boutros, M. (2014). Measuring genetic interactions in human cells by RNAi and imaging. Nat. Protoc. *9*, 2341–2353.

Lauschke, V.M., Tsiairis, C.D., François, P., and Aulehla, A. (2013). Scaling of embryonic patterning based on phase-gradient encoding. Nature *493*, 101–105.

Liberali, P., Snijder, B., and Pelkmans, L. (2014). A hierarchical map of regulatory genetic interactions in membrane trafficking. Cell *157*, 1473–1487.

Liberali, P., Snijder, B., and Pelkmans, L. (2015). Single-cell and multivariate approaches in genetic perturbation screens. Nat. Rev. Genet. *16*, 18–32.

Link, W., Oyarzabal, J., Serelde, B.G., Albarran, M.I., Rabal, O., Cebriá, A., Alfonso, P., Fominaya, J., Renner, O., Peregrina, S., et al. (2009). Chemical interrogation of FOXO3a nuclear translocation identifies potent and selective inhibitors of phosphoinositide 3-kinases. J. Biol. Chem. *284*, 28392–28400.

Liu, T., Sims, D., and Baum, B. (2009). Parallel RNAi screens across different cell lines identify generic and cell type-specific regulators of actin organization and cell morphology. Genome Biol. *10*, R26.

Loo, L.-H., Wu, L.F., and Altschuler, S.J. (2007). Image-based multivariate profiling of drug responses from single cells. Nat. Methods *4*, 445–453.

Lum, L., Yao, S., Mozer, B., Rovescalli, A., Von Kessler, D., Nirenberg, M., and Beachy, P.A. (2003). Identification of Hedgehog pathway components by RNAi in Drosophila cultured cells. Science *299*, 2039–2045.

Mayer, T.U., Kapoor, T.M., Haggarty, S.J., King, R.W., Schreiber, S.L., and Mitchison, T.J. (1999). Small molecule inhibitor of mitotic spindle bipolarity identified in a phenotype-based screen. Science *286*, 971–974.

Moffat, J., Grueneberg, D.A., Yang, X., Kim, S.Y., Kloepfer, A.M., Hinkle, G., Piqani, B., Eisenhaure, T.M., Luo, B., Grenier, J.K., et al. (2006). A lentiviral RNAi library for human and mouse genes applied to an arrayed viral high-content screen. Cell *124*, 1283–1298.

Mohr, S., Bakal, C., and Perrimon, N. (2010). Genomic screening with RNAi: results and challenges. Annu. Rev. Biochem. *79*, 37–64.

Montague, T.G., Cruz, J.M., Gagnon, J.A., Church, G.M., and Valen, E. (2014). CHOPCHOP: a CRISPR/Cas9 and TALEN web tool for genome editing. Nucleic Acids Res. *42*, W401–W407.

Morgan, T.H. (1910). Sex limited inheritance in Drosophila. Science *32*, 120–122.

Mullard, A. (2013). European lead factory opens for business. Nat. Rev. Drug Discov. *12*, 173–175.

Neumann, B., Held, M., Liebel, U., Erfle, H., Rogers, P., Pepperkok, R., and Ellenberg, J. (2006). High-throughput RNAi screening by time-lapse imaging of live human cells. Nat. Methods *3*, 385–390.

Neumann, B., Walter, T., Hériché, J.-K., Bulkescher, J., Erfle, H., Conrad, C., Rogers, P., Poser, I., Held, M., Liebel, U., et al. (2010). Phenotypic profiling of the human genome by time-lapse microscopy reveals cell division genes. Nature *464*, 721–727.

Nieland, T.J.F., Logan, D.J., Saulnier, J., Lam, D., Johnson, C., Root, D.E., Carpenter, A.E., and Sabatini, B.L. (2014). High content image analysis identifies novel regulators of synaptogenesis in a high-throughput RNAi screen of primary neurons. PLoS ONE *9*, e91744.

Nir, O., Bakal, C., Perrimon, N., and Berger, B. (2010). Inference of RhoGAP/GTPase regulation using single-cell morphological data from a combinatorial RNAi screen. Genome Res. *20*, 372–380.

Nüsslein-Volhard, C., and Wieschaus, E. (1980). Mutations affecting segment number and polarity in Drosophila. Nature *287*, 795–801.

Orvedahl, A., Sumpter, R., Jr., Xiao, G., Ng, A., Zou, Z., Tang, Y., Narimatsu, M., Gilpin, C., Sun, Q., Roth, M., et al. (2011). Image-based genome-wide siRNA screen identifies selective autophagy factors. Nature *480*, 113–117.

Otsu, N. (1979). A threshold selection method from gray-level histograms. IEEE Trans. Syst. Man Cybern. *9*, 62–66.

Pau, G., Fuchs, F., Sklyar, O., Boutros, M., and Huber, W. (2010). EBImage—an R package for image processing with applications to cellular phenotypes. Bioinformatics *26*, 979–981.

Ramadan, N., Flockhart, I., Booker, M., Perrimon, N., and Mathey-Prevot, B. (2007). Design and implementation of high-throughput RNAi screens in cultured Drosophila cells. Nat. Protoc. *2*, 2245–2264.

Ran, F.A., Hsu, P.D., Wright, J., Agarwala, V., Scott, D.A., and Zhang, F. (2013). Genome engineering using the CRISPR-Cas9 system. Nat. Protoc. *8*, 2281–2308.

Rank, K., and Unbehauen, R. (1992). An adaptive recursive 2-D filter for removal of Gaussian noise in images. IEEE Trans. Image Process. *1*, 431–436.

Rämö, P., Drewek, A., Arrieumerlou, C., Beerenwinkel, N., Ben-Tekaya, H., Cardel, B., Casanova, A., Conde-Alvarez, R., Cossart, P., Csúcs, G., et al. (2014). Simultaneous analysis of large-scale RNAi screens for pathogen entry. BMC Genomics *15*, 1162.

Roguev, A., Talbot, D., Negri, G.L., Shales, M., Cagney, G., Bandyopadhyay, S., Panning, B., and Krogan, N.J. (2013). Quantitative genetic-interaction mapping in mammalian cells. Nat. Methods *10*, 432–437.

Roy, A., McDonald, P.R., Sittampalam, S., and Chaguturu, R. (2010). Open access high throughput drug discovery in the public domain: a Mount Everest in the making. Curr. Pharm. Biotechnol. *11*, 764–778.

Sailem, H.Z., Sero, J.E., and Bakal, C. (2015). Visualizing cellular imaging data using PhenoPlot. Nat. Commun. *6*, 5825.

Schindelin, J., Arganda-Carreras, I., Frise, E., Kaynig, V., Longair, M., Pietzsch, T., Preibisch, S., Rueden, C., Saalfeld, S., Schmid, B., et al. (2012). Fiji: an open-source platform for biological-image analysis. Nat. Methods *9*, 676–682.

Scott, C.C., Vossio, S., Vacca, F., Snijder, B., Larios, J., Schaad, O., Guex, N., Kuznetsov, D., Martin, O., Chambon, M., et al. (2015). Wnt directs the endosomal flux of LDL-derived cholesterol and lipid droplet homeostasis. EMBO Rep. *16*, 741–752.

Sepp, K.J., Hong, P., Lizarraga, S.B., Liu, J.S., Mejia, L.A., Walsh, C.A., and Perrimon, N. (2008). Identification of neural outgrowth genes using genome-wide RNAi. PLoS Genet. *4*, e1000111.

Shalem, O., Sanjana, N.E., and Zhang, F. (2015). High-throughput functional genomics using CRISPR-Cas9. Nat. Rev. Genet. *16*, 299–311.

Simpson, J.C., Joggerst, B., Laketa, V., Verissimo, F., Cetin, C., Erfle, H., Bexiga, M.G., Singan, V.R., Hériché, J.-K., Neumann, B., et al. (2012). Genome-wide RNAi screening identifies human proteins with a regulatory function in the early secretory pathway. Nat. Cell Biol. *14*, 764–774.

Singh, S., Carpenter, A.E., and Genovesio, A. (2014). Increasing the content of high-content screening: an overview. J. Biomol. Screen. *19*, 640–650.

Snijder, B., Sacher, R., Rämö, P., Liberali, P., Mench, K., Wolfrum, N., Burleigh, L., Scott, C.C., Verheije, M.H., Mercer, J., et al. (2012). Single-cell analysis of population context advances RNAi screening at multiple levels. Mol. Syst. Biol. *8*, 579.

Sommer, C., and Gerlich, D.W. (2013). Machine learning in cell biology - teaching computers to recognize phenotypes. J. Cell Sci. *126*, 5529–5539.

St Johnston, D. (2002). The art and design of genetic screens: Drosophila melanogaster. Nat. Rev. Genet. *3*, 176–188.

Sundaramurthy, V., Barsacchi, R., Samusik, N., Marsico, G., Gilleron, J., Kalaidzidis, I., Meyenhofer, F., Bickle, M., Kalaidzidis, Y., and Zerial, M. (2013). Integration of chemical and RNAi multiparametric profiles identifies triggers of intracellular mycobacterial killing. Cell Host Microbe *13*, 129–142.

Tanenbaum, M.E., Gilbert, L.A., Qi, L.S., Weissman, J.S., and Vale, R.D. (2014). A protein-tagging system for signal amplification in gene expression and fluorescence imaging. Cell *159*, 635–646.

Thompson, G.C., Ireland, T.A., Larkin, X.E., Arnold, J., and Holsinger, R.M.D. (2014). A novel segmentation-based algorithm for the quantification of magnified cells. J. Cell. Biochem. *115*, 1849–1854.

Vizeacoumar, F.J., van Dyk, N., S Vizeacoumar, F., Cheung, V., Li, J., Sydorskyy, Y., Case, N., Li, Z., Datti, A., Nislow, C., et al. (2010). Integrating high-throughput genetic interaction mapping and high-content screening to explore yeast spindle morphogenesis. J. Cell Biol. *188*, 69–81.

Wang, X., Fu, A.Q., McNerney, M.E., and White, K.P. (2014). Widespread genetic epistasis among cancer genes. Nat. Commun. *5*, 4828.

Wang, Y.-L. (2007). Computational restoration of fluorescence images: noise reduction, deconvolution, and pattern recognition. Methods Cell Biol. *81*, 435–445.

Wheeler, D.B., Bailey, S.N., Guertin, D.A., Carpenter, A.E., Higgins, C.O., and Sabatini, D.M. (2004). RNAi living-cell microarrays for loss-of-function screens in Drosophila melanogaster cells. Nat. Methods *1*, 127–132.

Yin, Z., Sadok, A., Sailem, H., McCarthy, A., Xia, X., Li, F., Garcia, M.A., Evans, L., Barr, A.R., Perrimon, N., et al. (2013). A screen for morphological complexity identifies regulators of switch-like transitions between discrete cell shapes. Nat. Cell Biol. *15*, 860–871.

Young, D.W., Bender, A., Hoyt, J., McWhinnie, E., Chirn, G.-W., Tao, C.Y., Tallarico, J.A., Labow, M., Jenkins, J.L., Mitchison, T.J., and Feng, Y. (2008). Integrating high-content screening and ligand-target prediction to identify mechanism of action. Nat. Chem. Biol. *4*, 59–68.

Zhang, J.H., Chung, T.D., and Oldenburg, K.R. (1999). A simple statistical parameter for use in evaluation and validation of high throughput screening assays. J. Biomol. Screen. *4*, 67–73.